

ARTICLE

Supporting Information

Multi-Stimuli-Responsive Luminescent MCM48 Hybrid for Advanced Anti-Counterfeiting Applications

Leandro A. de Azevedo,^a Arturo Gamonal,^b Rosely Maier-Queiroz,^a Carolina S. Silva,^c Jamylle N. S. Ferro,^d Petrus d'Amorim S. C. Oliveira,^b Emiliano O. Barreto,^d Leonis L. da Luz*^b and Severino Alves Júnior.*^{a, b}

Chemicals

Cetyl bromide (CTAB) (Sigma aldrich, 98%), F127 (Pluronic®F-127) (Sigma aldrich), absolute ethanol (EtOH) (Merck, 99.9% PA), 29% ammonium hydroxide solution Sigma Aldrich, 98%), aminopropyl 3-(triethoxysilane) (APTES) and 3-Isocyanatopropyl 3-(Triethoxysilane) (TESPIC) (Sigma Aldrich, 95%), trimesic acid) (Sigma Aldrich, 95%), Dicyclohexylcarbodiimide (DCC) (Sigma Aldric, 99%), 4-dimethylaminopyridine (DMPA) (Sigma Aldrich, 99%), dimethylformamide (DMF) 1.21 mmol), (Sigma aldrich, 95%), Toluene, 4,4,4-trifluoro-1-phenyl-1,3-butadione (BTFA) and Ethylene glycol (Dynamic) (masterprint), Europium oxide (Sigma Aldric, 99%).

Synthesis of hybrid materials

The europium-complexes grafted onto mesoporous silica MCM-48 (SiO₂) were synthesized in four steps procedure following the experimental approach described by Li et al.²¹ and Fujiwara,²² respectively for grafting of trimesic and chelidamic acids. We starting by synthesizing the SiO₂ through modified Stöber method.²⁰ Then, were performed reaction of SiO₂ and H₂DAMIC with the coupling agent TESPC, respectively for H₂BTC-SiO₂ and H₂DAMIC-SiO₂. Next, trimesic and TESPIC-H₂DAMIC was covalently linked to silica, resulting in the H₂BTC-SiO₂ and H₂DAMIC-SiO₂ materials. Finally, the trivalent europium ions (Eu³⁺) were coordinated to the benzene-carboxylic (H₂BTC-SiO₂) and pyridine-carboxylic (H₂DAMIC-SiO₂) chelating groups, using europium nitrate aqueous solutions resulting in the luminescent hybrids Eu(H₂O)_nBTC-SiO₂ and Eu(H₂O)_nDAMIC-SiO₂.

Synthesis of MCM48 mesoporous silica

MCM48 was synthesized according methodology adapted from Kin, Chung et al.¹ In that approach 0.5g of cetyltrimethylammonium bromide (CTAB) was stirred with 2.05g of Pluronic®F Diluted in 96 mL of distilled water, 43 mL of absolute ethanol (ETOH) and 11 mL of 29% ammonium hydroxide solution. After complete dissolution of the reagents, 2 mL of Tetraethyl Orthosilicate (TEOS) was added and stirred for about 5 minutes, until the solution became whitish. The mixture was allowed to stand for 24 hours at room temperature for condensation of the silica. Subsequently, the sample was centrifuged using 6000 rpm for 40 min and washed 4 times with distilled water. A white precipitate was obtained and it was held at 70 °C for 24 hours, and then calcined at 550 °C in air for 4 hours to remove the organic phase.

Eu(H₂O)_nBTC-SiO₂ hybrid

Firstly, functionalization of MCM48 was performed with the coupling silane aminopropyl 3-(triethoxysilane) (APTES). This synthesis was adapted from the methodology of Saindulo Gangi and collaborators.² In that approach 100 mg of MCM48 were suspended in 10 mL of toluene, then 3 mL of APTES were added dropwise. The mixture was refluxed for 24 h at 120 °C. Subsequently, the suspension was precipitated by centrifugation at 6000 rpm, washed several times with toluene and dried at 60 °C for 6 hours. Finally, a white solid was obtained and called as H₂N-SiO₂. Afterward, 280 mg of the synthesized H₂N-SiO₂ was dispersed in 28 mL of DMF, then 260 mg (1.23 mmol) of H₃BTC, 260 mg (1.26 mmol) Dicyclohexylcarbodiimide (DCC) and 15.3 mg (0.1 mmol) 4-dimethylaminopyridine (DMPA) was following added. This mixture was refluxed under nitrogen atmosphere and heating (100 °C) for 36 hours. Subsequently, the system was centrifuged at 6000 rpm and the precipitate washed in DMF, water and absolute ethanol in the ratio of 1:1:4, respectively. Finally, the powder was washed with acetone. The solid, light brown,

corresponding to the H₂BTC-SiO₂ hybrid, was dried at 60 °C under vacuum for 5 hours. The last step was the coordination of Eu³⁺ ions with chelating groups of the H₂BTC-SiO₂ material. To do this, europium nitrate (0.1, 0.2, and 0.3 mmol) was solubilized in 3 ml of distilled water using a borosilicate microwave reactor (10 ml). Then, 50 mg of H₂BTC-SiO₂ was dispersed in this solutions and heated at 140 °C in a microwave (100 W) for 20 minutes.³ At the end, the samples were centrifuged and washed with water 5 times and drying in vacuum oven at 60 °C for 5h.

Eu(H₂O)_nDAMIC-SiO₂ hybrid

The synthetic approach for graft H₂DAMIC to SiO₂ is somewhat different from used for the H₃BTC. Here we have used the protocol developed by Fujiwara et al with some modifications.² Firstly, 0.222 g (1.21 mmol) of H₂DAMIC, 0.300 g (1.21 mmol) of 3-(triethoxysilyl) propylisocyanate (TESPIC) and 1.5 mL of DMF was stirred and refluxed at 120 °C for 24 h. Then, 0.5 mL of dry toluene suspension and M mg of SiO₂ were added to this system and refluxed for a further 24 h. Afterward, the H₂DAMIC-SiO₂ was collected by centrifugation (6000 rpm) and washed 3 times with 1:1 DMF/toluene to give a white solid, in which was dried at 70 °C under vacuum for 5 hours. The complexation step with Eu³⁺ ions was carried out from europium nitrate dissolution in 3 ml of distilled water using a borosilicate microwave reactor with a capacity of 10 ml. Then, 50 mg of H₂DAMIC-SiO₂ was dispersed in this solutions and heated at 140 °C in a microwave (100 W) for 20 minutes.⁴ Finally, the Eu(H₂O)_nDAMIC-SiO₂ hybrid was collected by centrifuged and washed with water 5 times and drying in vacuum oven at 60 °C for 5h.

Amount of Eu³⁺ loaded

The quantifications of the Eu³⁺ loaded in the hybrids (**Table S2**) were carried out via complexometric titration with ethylene diamine tetraacetic acid (EDTA) 0.01 mol.L⁻¹. After complexation step and centrifugation, 1mL of the supernatants and 0.5 mL of the orange xylenol indicator were mixed. Next, the titration was performed using EDTA solution up to the sample color change from red-violet to yellowish (equivalence point).

Both hybrids showed amount saturation of Eu³⁺ ions equal to ca. 0.01 mmol on each 50 mg of material. This indicates that Eu(H₂O)_nBTC-SiO₂ hybrid shows a smaller concentration of chelating agent once that the stoichiometric proportion Eu³⁺/chelating are 1:1 for Eu(H₂O)_nDAMIC-SiO₂ and 2:1 for Eu(H₂O)_nBTC-SiO₂.

Table S1. Amount of Eu³⁺ in 50 mg of the SiO₂.

Hybrid	Amount of Eu ³⁺ (mmol)
Eu(H ₂ O) _n BTC-MCM48	0.02
	0.10
	0.09
Eu(H ₂ O) _n DAMIC-MCM48	0.04
	0.12
	0.11

Anticounterfeit ink preparation

The anticounterfeiting inks were obtained by dispersion of 3.0 mg of Eu(H₂O)_nBTC-SiO₂ and Eu(H₂O)_nDAMIC-SiO₂ in 10 mL of a mixture of monoethyleneglycol/ethanol, 93:7, using ultrasound probe for 30 min (180 W, 40 KHz). Then, the homogeneous dispersion was introduced into a cartridges and the optimized printer parameters were set according to **Table S4**.

In vitro assay

Cell Culture

3T3 fibroblast were cultured in Dulbecco's Modified Eagle Medium (DMEM) containing 10% fetal bovine serum (FBS), L-glutamine (2 mM) and gentamicin (40 µg/mL) in a humidified incubator in atmosphere with 5% CO₂ at 37°C.

Human lung epithelial cells (A549), a cell line, were cultured in RPMI-1640 supplemented with 10% SBF, L-glutamine (2 mM) and 40 µg/mL gentamicin. For treatments, the cells were cultured in serum-free medium.

Cell viability Assay

The effect of MCM48, BTFA, NH₂-MCM48, H₂BTC-SiO₂, Eu(H₂O)_nBTC-SiO₂, H₂DAMIC-SiO₂, Eu(H₂O)_nDAMIC-SiO₂, Eu(BTFA)₃BTC-SiO₂, Eu(BTFA)₃DAMIC-SiO₂ and TTA on A549 and 3T3 cell viability was performed by MTT assay (MOSMANN, 1983).⁵

Briefly, the cells were seeded in a 96-well plate (A549 1 × 10⁴ or 3T3 7 × 10³ cells/well) overnight and treated with different concentration of the samples (3, 30, 100 or 300 µg/mL) for 24 hours.

After the incubation with the treatment, 22.5 µL of MTT (3-(4,5-dimethylthiazol-2-yl)-2,5-diphenyltetrazolium bromide) (Sigma-Aldrich – EUA) (5 mg/mL in PBS) was added to each well for 3 hours. Then, the supernatant was discarded and 150 µL of DMSO was added to each well to solubilize the formed formazan crystals. The absorbance of each well was recorded using a microplate spectrophotometer and the optical density (OD) was measured at 540 nm. The percentage of viability cell was calculated through this formula: (OD treated cells/OD non-treated cells) × 100.

Equipment

The Fourier Transform Infrared Analysis were performed in a Perkin Elmer device, model Spectrum 400, in the region of 4000–400 cm⁻¹ with UATR accessory (Universal sampling accessory with pressure arm). The spectra had a resolution of 2 cm⁻¹ to 32 accumulations. The measurements were carried out at room temperature in the Fuel Laboratory (LAC), in the Department of Chemical Engineering (DEQ), UFPE. Porosimetry was performed in the Micromeritics Model ASAP 2420. The equipped has 12 independent sample treatment stations and 6 analysis stations operating simultaneously.

The XRD, The measurements were performed on a Rigaku diffractometer, model RINT 2000 / PC, which uses Cu K rad radiation. The diffraction patterns for the angular range 2θ = 1°–9° to obtain the MCM48 standards, in continuous scan module with step of 0,01°, with a speed of 1 min with a counting time of 1 second. The scanning electron microscopy (SEM) was obtained TESCAN MIRA's 4th generation with FEG Schottky electron emission source combines SEM imaging and live elemental composition analysis. To perform SEM and elemental analysis, the powder samples were capped with a gold film. The samples was previously coated with gold film by sputtering coater. To perform EDS and FTIR analysis of Eu(BTFA)₃SiO₂ hybrids, after soaking hydrated samples in BTFA solution and then, the samples were dispersed in ethanol under stirring for 30 min. Next, the powder was collected by centrifugation. This wash procedure was performed for three times. After drying in ambient conditions, the samples were analyzed. The thermogravimetric-TGA analysis was obtained in the equipment manufactured by Shimadzu model DTG-60H with the analysis parameters in the range of 10 °C per minute in nitrogen atmosphere. Emission and excitation and lifetime spectra were performed in a Horiba Jobin Yvon, Fluorolog-3 ISA spectrofluorimeter. The values for lifetime are determined by fitting the luminescence decay curve to the function $I = I_0 e^{-t/\tau} + b$.

Quantum Yield (Q_{Ln}^{Ln}) calculation

The intrinsic emission quantum yield (Q_{Ln}^{Ln}) of the ⁵D₀ emitting level is defined by the ratio between the radiative emission and total decay rates (radiative and non-radiative) for this particular energy level, according to follows equation.⁴

$$Q_{Eu}^{Eu} = \frac{A_{rad}}{A_{rad} + A_{nrad}}$$

The total decay rate ($A_{rad} + A_{nrad}$) is related to the deactivation process of the ⁵D₀ level, mainly by multiphoton relaxation, which is determined by the experimental lifetime values as follows:

$$\frac{1}{A_{rad} + A_{nrad}} = \frac{1}{A_{Total}} = \frac{1}{\tau}$$

In these equations, A_{rad} and A_{nrad} are the radiative and non-radiative spontaneous emission coefficients of ⁵D₀ → ⁷F_J transitions (J = 1, 2 and 4) of the Eu³⁺ ion. A_{rad} coefficient values were determined by $A_{rad} = \sum A_{0 \rightarrow J}$ where $A_{0 \rightarrow J}$ are the spontaneous emission coefficients of ⁵D₀ → ⁷F_J transitions (J = 1, 2 and 4) of the Eu³⁺ ion. $A_{0 \rightarrow J}$ are determined by

$$A_{0 \rightarrow j} = A_{0 \rightarrow 1} \left(\frac{S_{0 \rightarrow j}}{S_{0 \rightarrow 1}} \right)$$

Where $S_{0 \rightarrow j}$ are the integrated areas under the emission curves. The spontaneous emission coefficient $A_{0 \rightarrow 1}$ of the ${}^5D_0 \rightarrow {}^5F_1$ transition is mostly ruled by the magnetic dipole mechanism and depends only on the refractive index of the material. Therefore, this transition is taken as a reference.⁴

FTIR Discussion

The success of graft reaction steps were monitored through FTIR spectroscopy (**Figure S1**). FT-IR spectrum for unmodified SiO_2 showed characteristic band at 1052 and 792 cm^{-1} assigned to the Si–O–Si and Si–O stretching vibrations, respectively (Black lines of Figure S1a). Also, the broadband in the region between 3,000 and 3,700 cm^{-1} corresponds to the stretching of the O–H bond of the silane hydroxyl groups and water molecules adsorbed on the mesoporous materials.⁶ The functionalization of surface of the SiO_2 with amine groups on the surface was confirmed by additional peaks at 1560 and in the region of 3377–3120 cm^{-1} assigned to the NH_2 scissoring and stretching of the N–H bond (blue line of Figure S1a).⁷ Moreover, characteristic peaks of the C–H stretching of the methylene groups of the TESPIC coupling agent in the range of 3023–2760 cm^{-1} are further evidence of the successful functionalization. After reaction with H_3BTC , the FTIR spectrum (green line of Figure S1a) showed new bands at ca. 1560 and 1660 cm^{-1} related to C=O of acid and amide groups indicating that chelating ligand has been successfully grafted onto $\text{NH}_2\text{-SO}_2$. Also, a small band assigned to N–H stretching of the secondary amide group is observed at 3275 cm^{-1} . These results unambiguously confirmed the mechanism displayed in the Scheme 1a. The coordination of the metal ions Eu^{3+} is evidenced by the shift of the -40 cm^{-1} in the energy of signal of the $\nu_{\text{as}}(\text{COO}^-)$ regarding $\nu_{\text{s}}(\text{C=O})$ signal of protonated $\text{H}_2\text{BTC-SiO}_2$. In addition, the energy of $\nu_{\text{as}}(\text{COO}^-)$ and $\nu_{\text{s}}(\text{COO}^-)$ are typical of the chelate bidentate mode of the carboxylic group of the BTC.^{5,6,7} On the other hand, after consecutive reactions between TESPIC, H_2DAMIC and SiO_2 , in that order, in the FTIR of the resulting material $\text{H}_2\text{DAMIC-SiO}_2$ (Figure S1b) the disappearing of the N=C=O stretch vibration peak at 2,270 cm^{-1} for TESPIC and the emergence of N–H stretching of secondary amide group at 3,300 cm^{-1} indicates that H_2DAMIC has been grafted on to TESPIC.^{8,9} In addition, the Si–C stretching vibration located at ca. 1,211 cm^{-1} , and the stretching vibration band of Si–O at 1,052 cm^{-1} reveal the existence of the siloxane bonds. As well as for $\text{Eu}(\text{H}_2\text{O})_n\text{BTC-SiO}_2$, the coordination of the metal ions Eu^{3+} is evidenced by the shift of energy of $\nu_{\text{as}}(\text{COO}^-)$ of the 81 cm^{-1} regarding $\nu_{\text{s}}(\text{C=O})$ signal of protonated $\text{H}_2\text{DAMIC-SiO}_2$ hybrid. In addition, the energy of $\nu_{\text{as}}(\text{COO}^-)$ and $\nu_{\text{s}}(\text{COO}^-)$ is typical for the chelate tridentate mode of the carboxylic group of the DAMIC.⁸

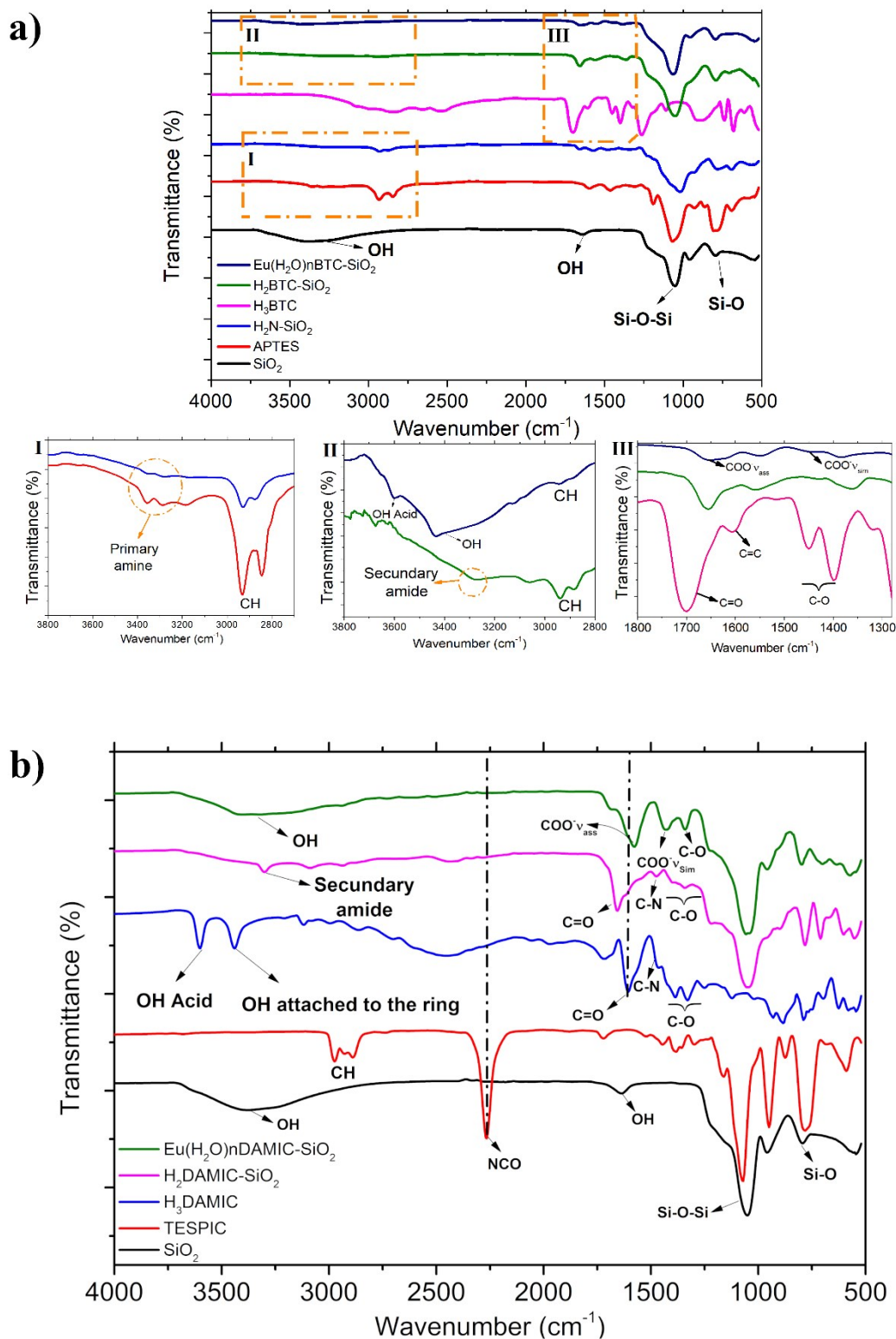


Figure S1: FTIR spectra of (a) SiO₂, APTES, H₃BTC, H₂N-SiO₂, H₂BTC-SiO₂, Eu(H₂O)_nBTC-SiO₂ and (b) SiO₂, TESPIC, H₂DAMIC, H₂DAMIC-SiO₂, Eu(H₂O)_nDAMIC-SiO₂.

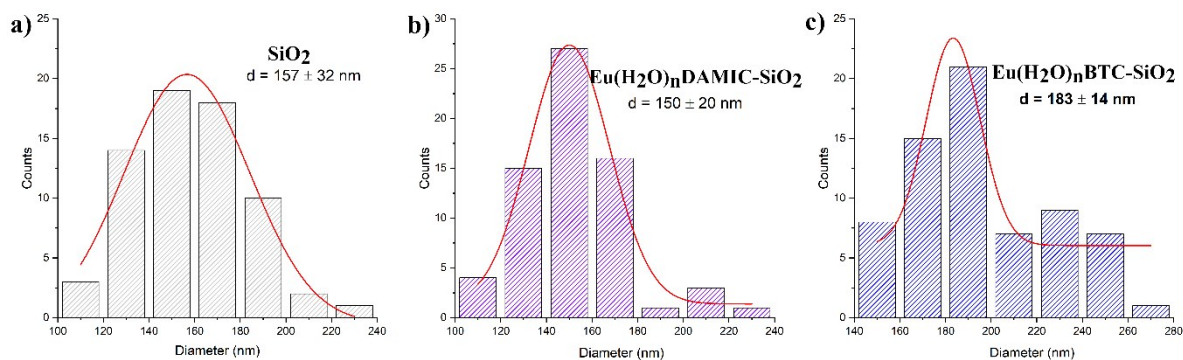


Figure S2: Particle distribution histogram of MCM48, $\text{Eu}(\text{H}_2\text{O})_n\text{BTC-SiO}_2$ and $\text{Eu}(\text{H}_2\text{O})_n\text{DAMIC-SiO}_2$.

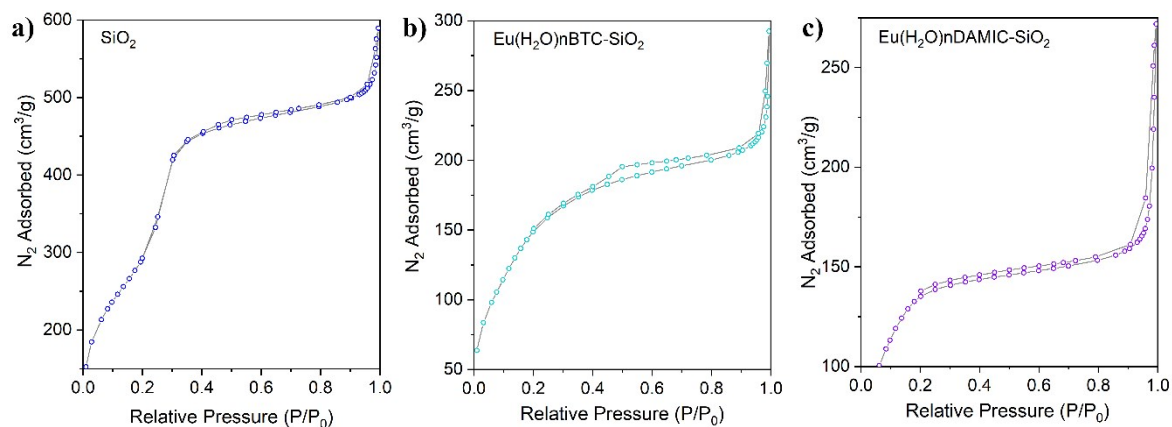


Figure S3. Nitrogen adsorption–desorption isotherms for MCM48 and hybrids $\text{Eu}(\text{H}_2\text{O})_n\text{BTC-SiO}_2$ and $\text{Eu}(\text{H}_2\text{O})_n\text{DAMIC-SiO}_2$.

Table S2. Porosimetry of MCM48 and hybrids EuBTC-MCM48 and EuDAMIC-MCM48 .

Materials	Surface area m^2/g	Pore volume cm^3/g
MCM48	1,070.6	0.973
$\text{Eu}(\text{H}_2\text{O})_n\text{BTC-SiO}_2$	578.8	0.386
$\text{Eu}(\text{H}_2\text{O})_n\text{DAMIC-SiO}_2$	499.5	0.388

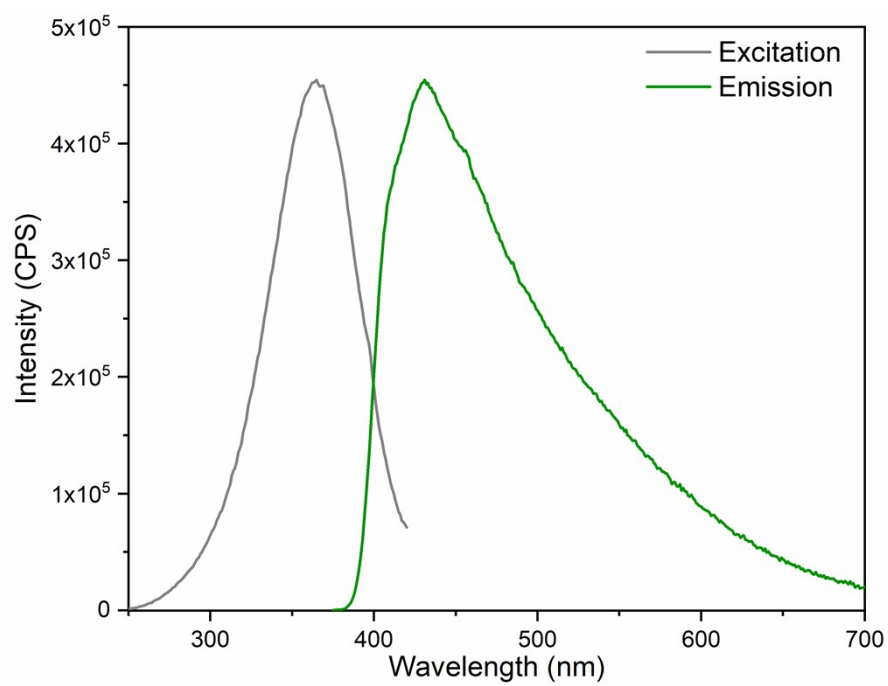


Figure S4. Excitation ($\lambda_{Em} = 437$ nm) and emission ($\lambda_{Ex} = 362$ nm) spectra of the SiO₂.

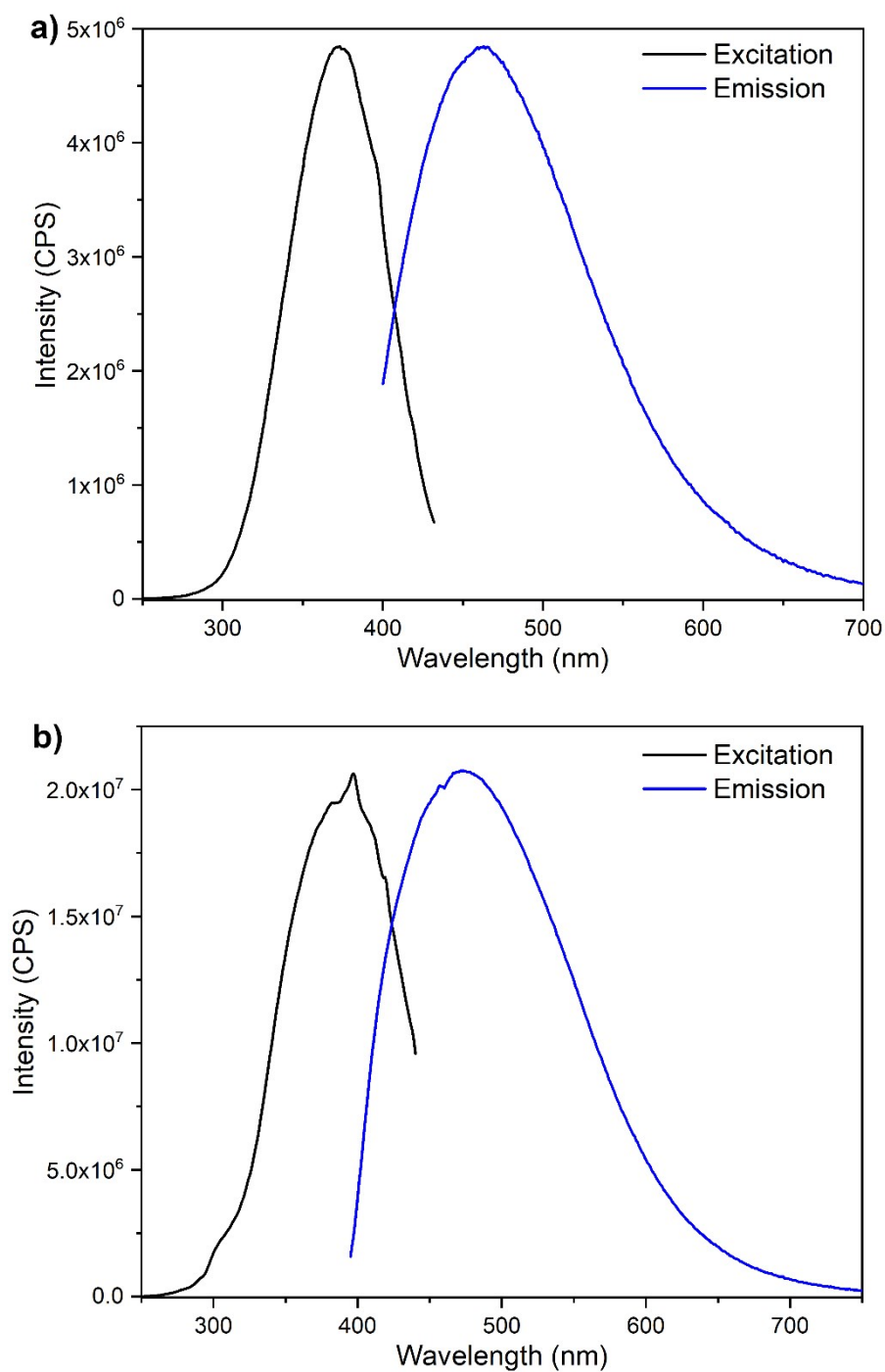


Figure S5. Excitation and emission spectra of the (a) H₂DAMIC-SiO₂ ($\lambda_{Em} = 442$ nm $\lambda_{Ex} = 375$ nm) and (b) H₃BTC-SiO₂ ($\lambda_{Em} = 470$ nm $\lambda_{Ex} = 382$ nm).

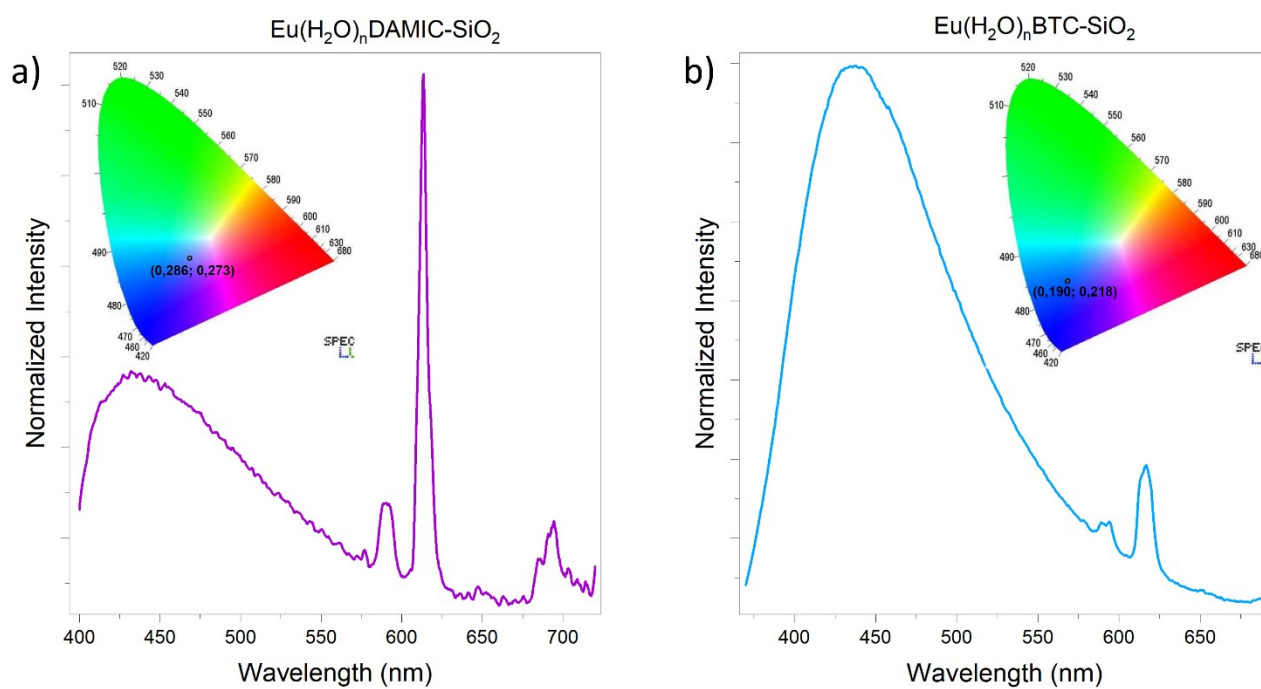


Figure S6. Emission spectra ($\lambda_{\text{ex}} = 365$ nm) and corresponding chromaticity diagram of (a) $\text{Eu}(\text{H}_2\text{O})_n\text{DAMIC-SiO}_2$ b) $\text{Eu}(\text{H}_2\text{O})_n\text{BTC-SiO}_2$.

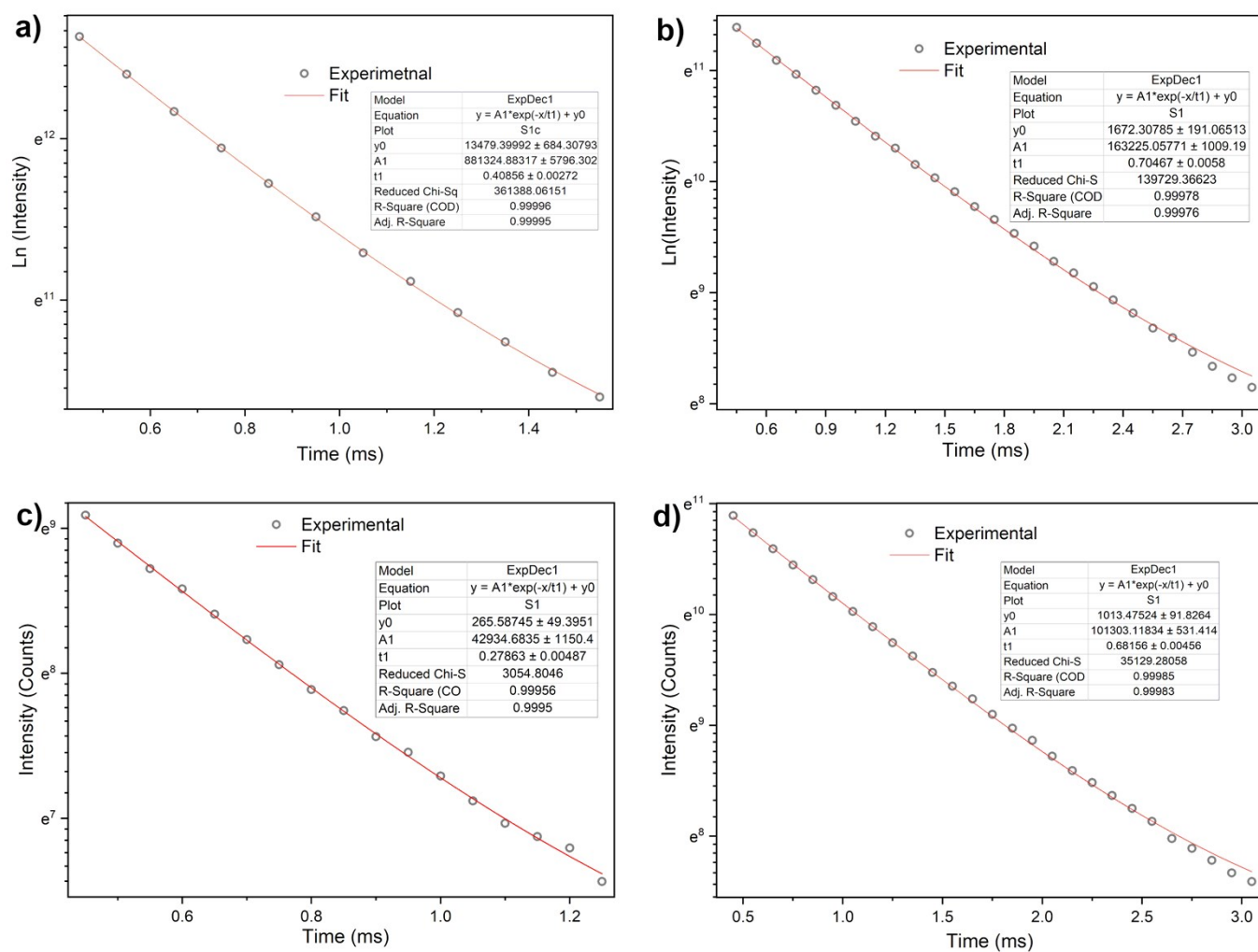


Figure S7. Luminescence decay curves of the (a) $\text{Eu}(\text{H}_2\text{O})_n\text{DAMIC-SiO}_2$ ($\lambda_{\text{Ex}} = 312 \text{ nm}$, $\lambda_{\text{Em}} = 618 \text{ nm}$), b) $\text{Eu}(\text{BTFA})_3\text{DAMIC-SiO}_2$ ($\lambda_{\text{Ex}} = 355 \text{ nm}$, $\lambda_{\text{Em}} = 612 \text{ nm}$), c) $\text{Eu}(\text{H}_2\text{O})_n\text{BTC-SiO}_2$ ($\lambda_{\text{Ex}} = 292 \text{ nm}$, $\lambda_{\text{Em}} = 616 \text{ nm}$) and d) $\text{Eu}(\text{BTFA})_3\text{DAMIC-SiO}_2$ ($\lambda_{\text{Ex}} = 370 \text{ nm}$, $\lambda_{\text{Em}} = 611 \text{ nm}$).

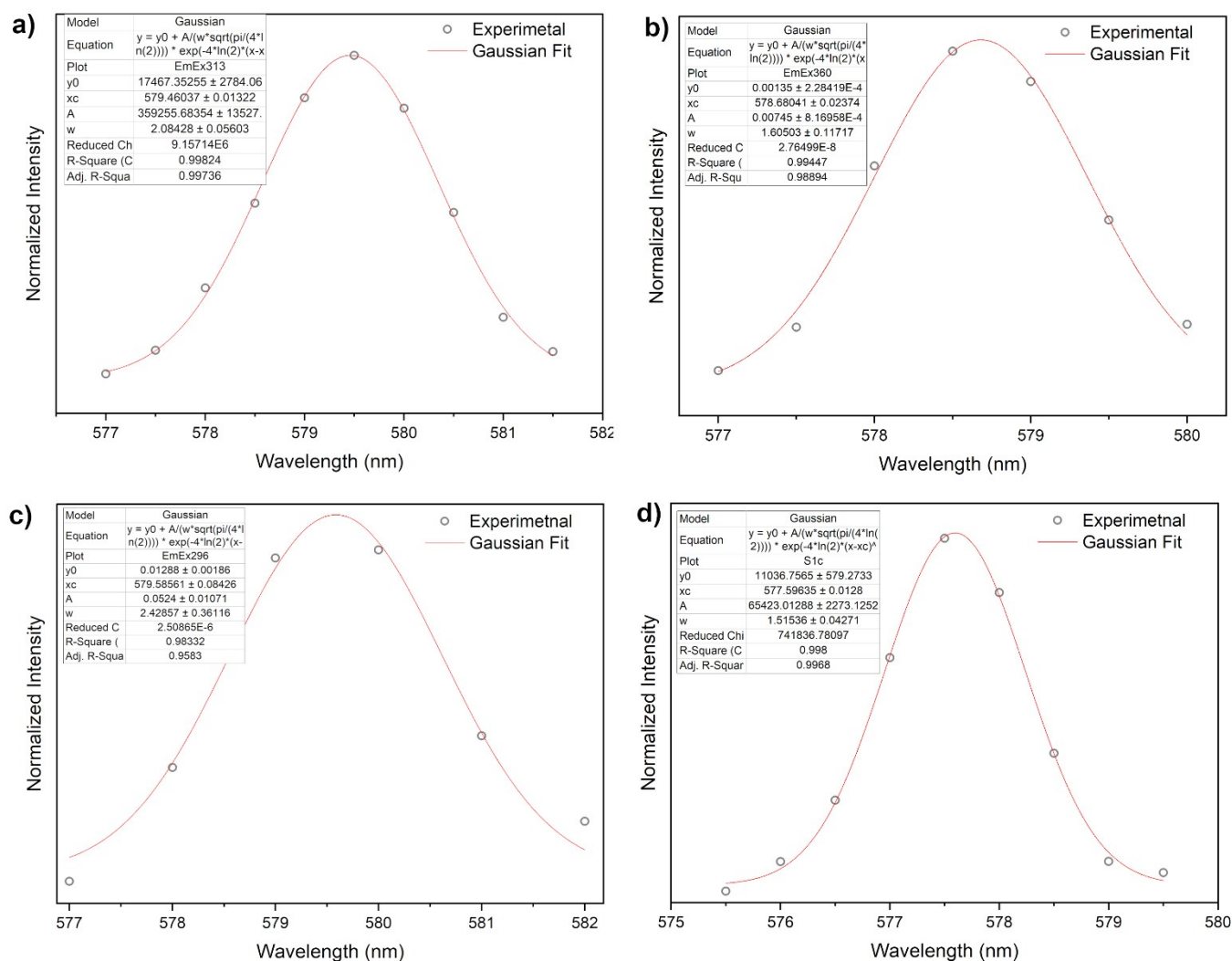


Figure S8. Emission spectra and Gaussian fit of the ⁵D₀ → ⁷F₀ of the (a) Eu(H₂O)_nDAMIC-SiO₂, b) Eu(BTFA)₃DAMIC-SiO₂, c) Eu(H₂O)_nBTC-SiO₂ and d) Eu(BTFA)₃DAMIC-SiO₂.

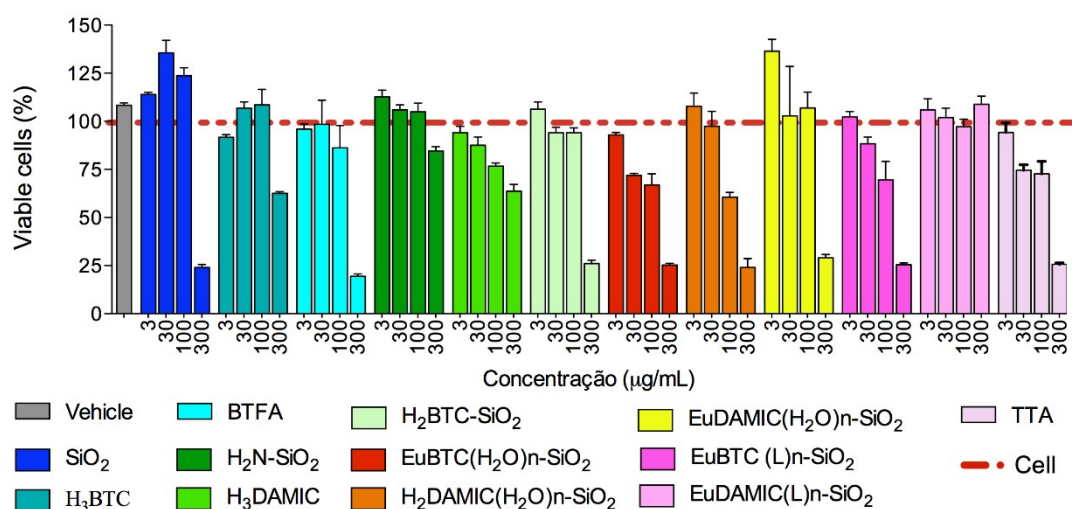
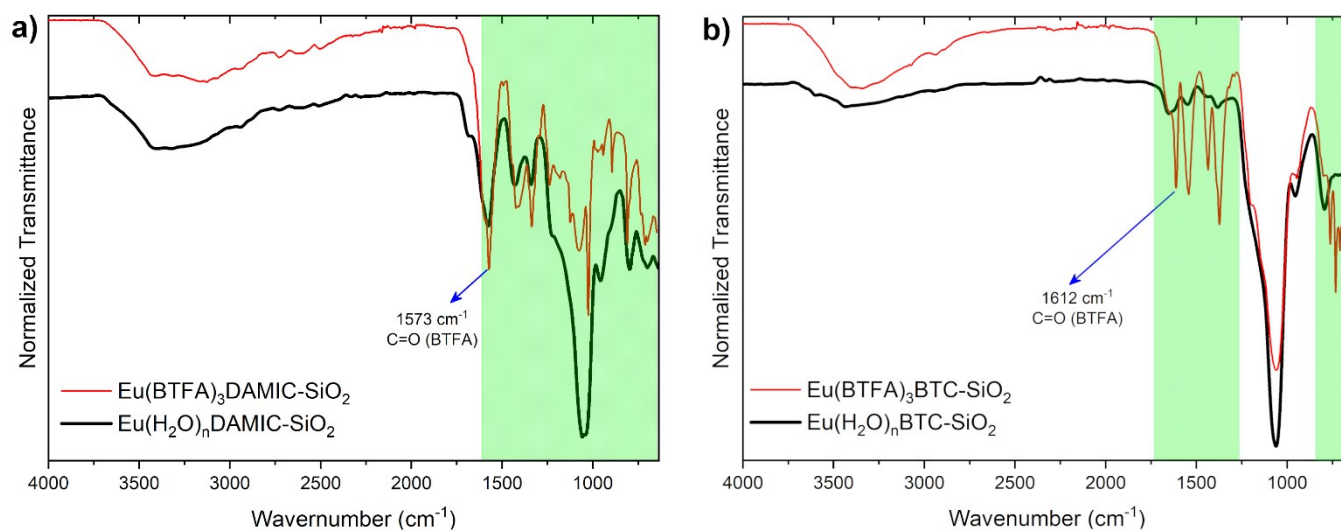


Figure S9. Effects on 3T3 cell viability (24 hours). The bars represent the mean ± SEM. The dashed line represents the control group (treated with DMEM). The group vehicle represent the treatment with ethanol 0.001%. Data were expressed as % viable cells compared to the control group. One-way ANOVA followed by the Newman-Keuls post-test, ** p < 0.01 and *** p < 0.001 (Control vs. treatment).

Table S3. Integrated intensity, $R[I(^5D_0 \rightarrow ^7F_2)]/[I(^5D_0 \rightarrow ^7F_1)]$, ratio of the powders of the hybrids

Material	$R[I(^5D_0 \rightarrow ^7F_2)]/[I(^5D_0 \rightarrow ^7F_1)]$
Eu(H₂O)_nBTC-SiO₂	5.5
Eu(BTFA)₃BTC-SiO₂	12.5
Eu(H₂O)_nDAMIC-SiO₂	5.1
Eu(BTFA)₃DAMIC-SiO₂	16.8

**Figure S10.** FTIR spectra of (a) Eu(H₂O)_nDAMIC-SiO₂ and Eu(BTFA)₃DAMIC-SiO₂, and b) Eu(H₂O)_nBTC-SiO₂ and Eu(BTFA)₃BTC-SiO₂.**Table S4.** Elemental quantitative analysis with the mass percentage obtained by EDS for the Eu(BTFA)₃L-SiO₂ hybrids, L = BTC or DAMIC.

Material		Eu (%)	F (%)
Eu(BTFA)₃BTC-SiO₂	Experimental	7.6	28.4
	Calculated	72.7	27.3
Eu(BTFA)₃DAMIC-SiO₂	Experimental	70.6	29.4
	Calculated	72.7	27.3

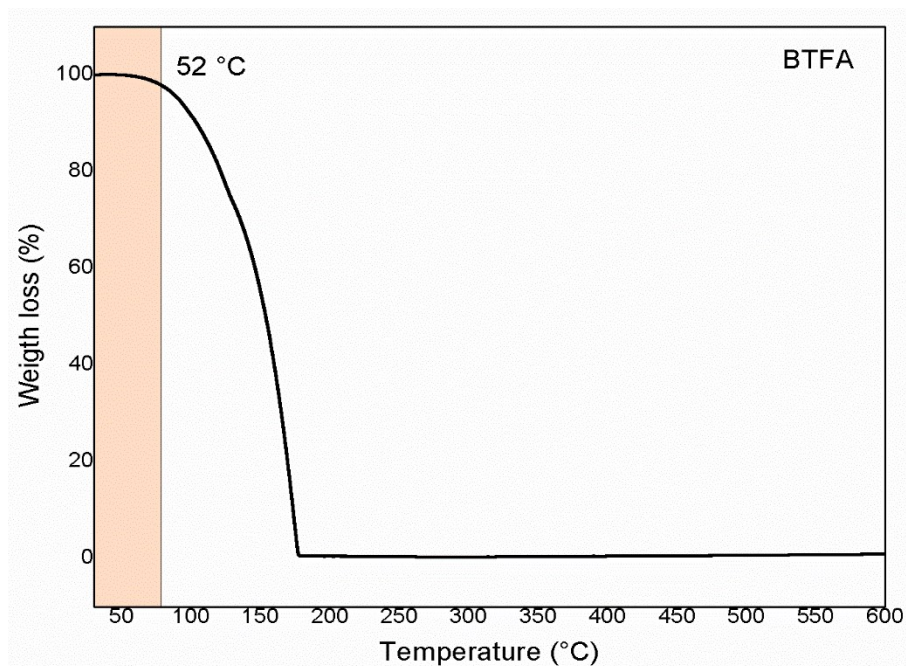


Figure S11. BTFA thermogravimetric analysis

Table S4. Parameters used in the print and cleaning cartridges for the compounds EuBTC-MCM48 and EuDAMIC-MCM48

Parameters	EuBTC-MCM48 and EuDAMIC-MCM48
DDP [V]	15
Fmax [kHz]	20
Cartridge temperature [°C]	30°C
Cleaning Cycles (spt-spt)	Purge.3 secs after 25 bands
Plate temperature [°C]	28
Waiting time between subsequent layers (> 10 layers) [s]	90 second per deposition
Waiting time between subsequent layers (> 20 layers) [s]	120 second per deposition

Table S5. Parameters for control algorithms

Control phase	Level	Slope	Duration
DDP constant	3.584 μ s	9.472 μ s	26.816 μ s
Fluid ejection	5.056 μ s	20.416 μ s	26.816 μ s

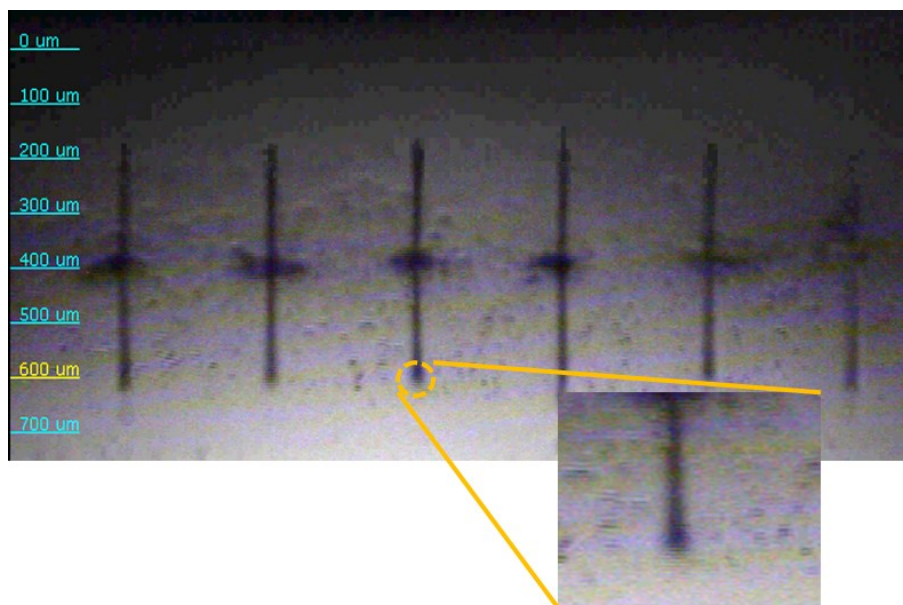


Figure S12. Image taken by the Fiducial Camera tool of security ink being ejected under a DoD printhead.

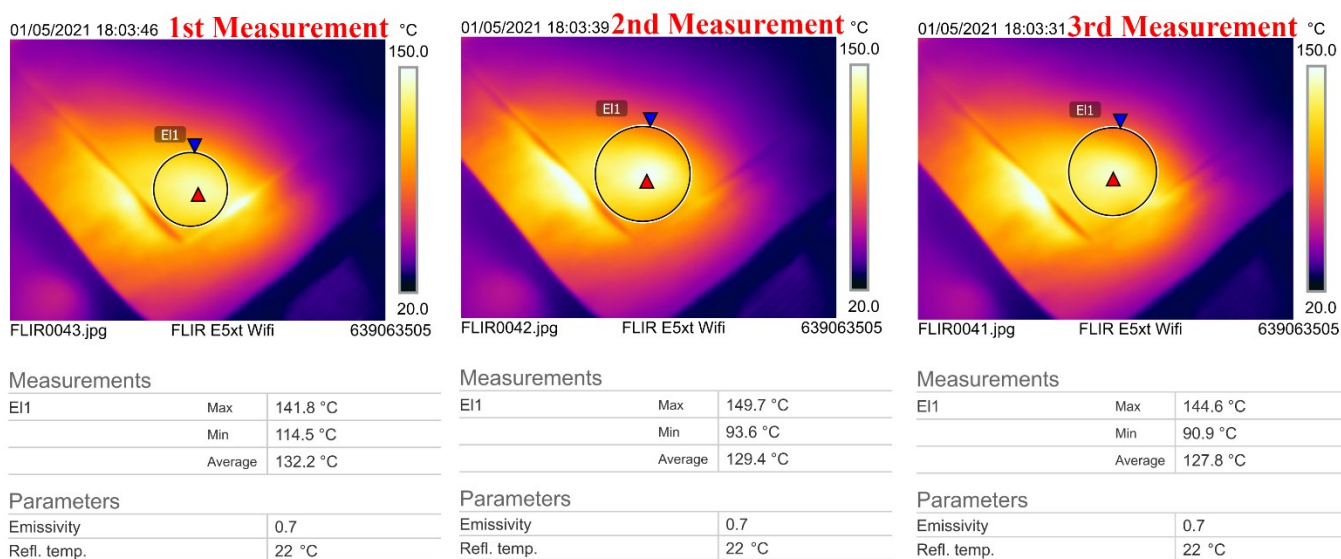


Figure S13. Thermal images of a sample of printed label heated during luminescence quenching experiment.

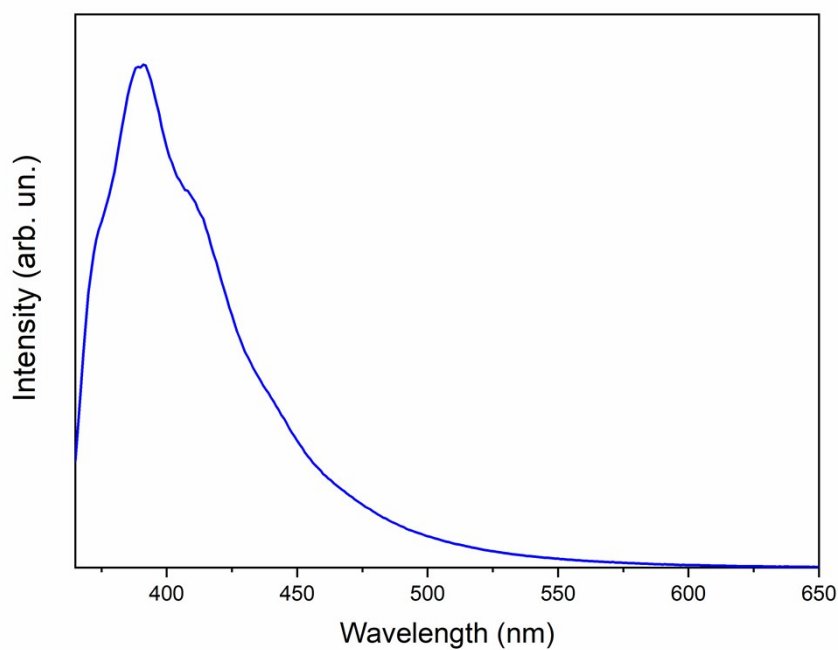


Figure S14. Emission spectra ($\lambda_{\text{ex}} = 342 \text{ nm}$) of the BOP.

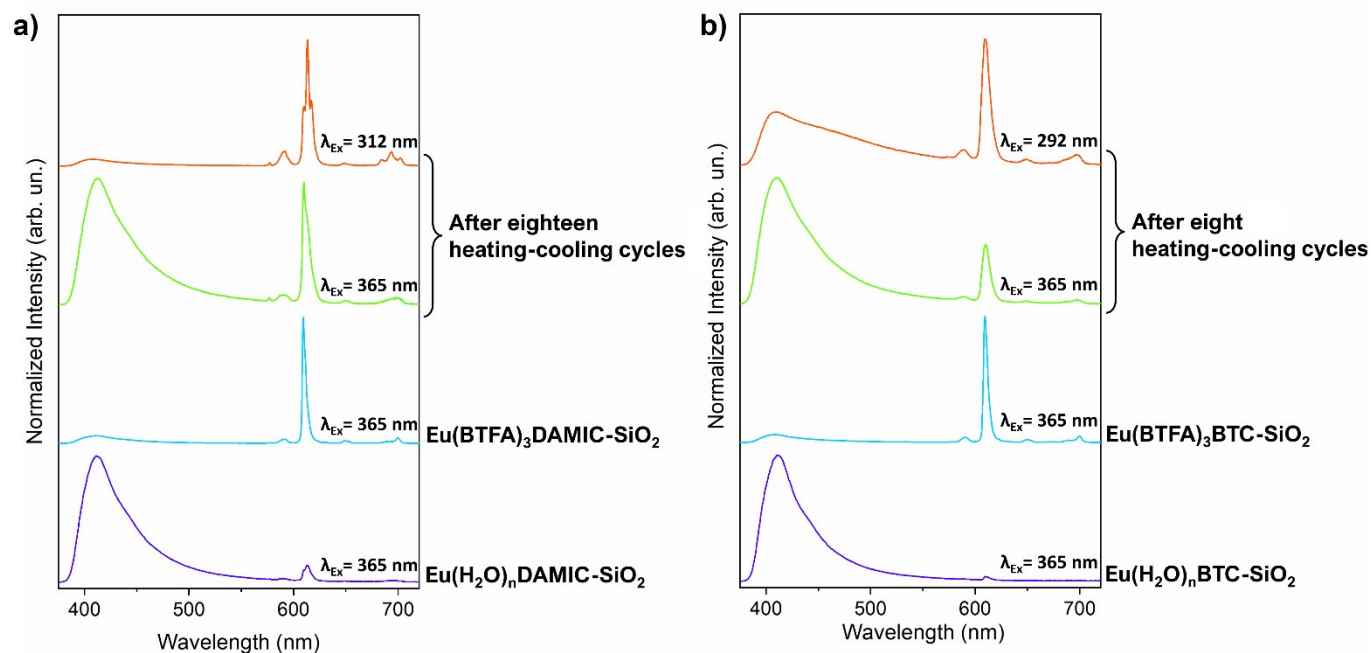


Figure S15. Emission spectra of the a) UFPE and b) BSTR labels before, after soak with BTFA and after heating cycles.

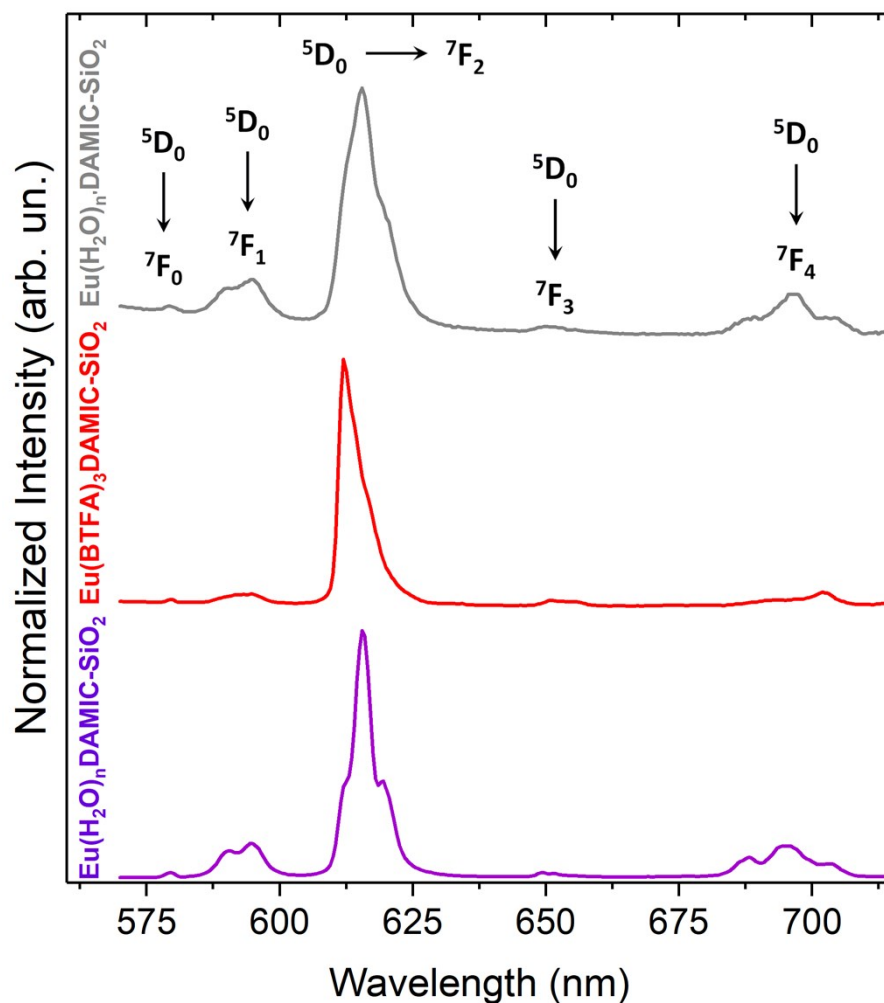


Figure S16. Emission spectra ($\lambda_{\text{ex}} = 365 \text{ nm}$) of $\text{Eu}(\text{L})\text{DAMIC-SiO}_2$ as-printed (purple line), after soak with BTFA (red line) and after heating (gray line).

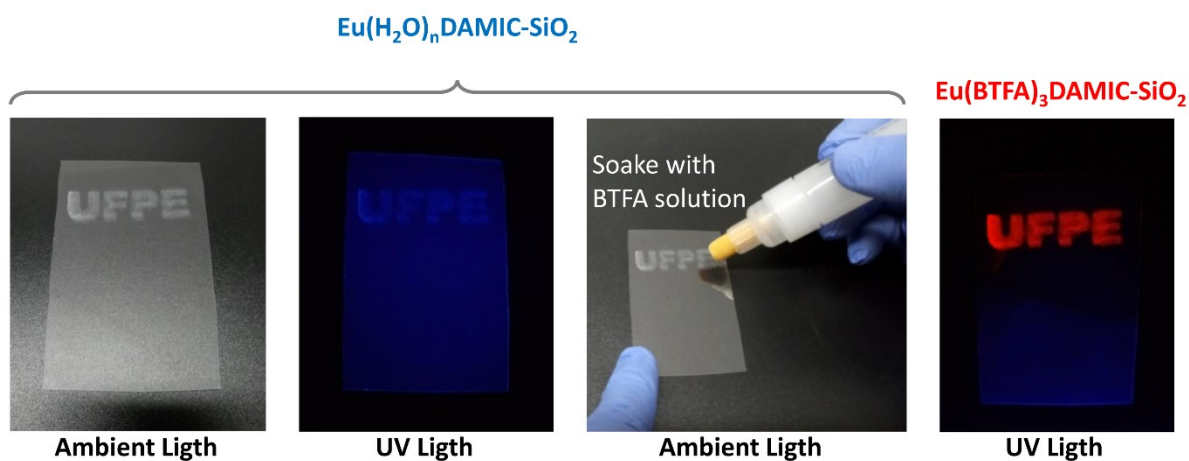


Figure S17. Procedure of bright red luminescence ON of the printed security label "UFPE" and its luminescence with a UV light with wavelength of 365 nm.

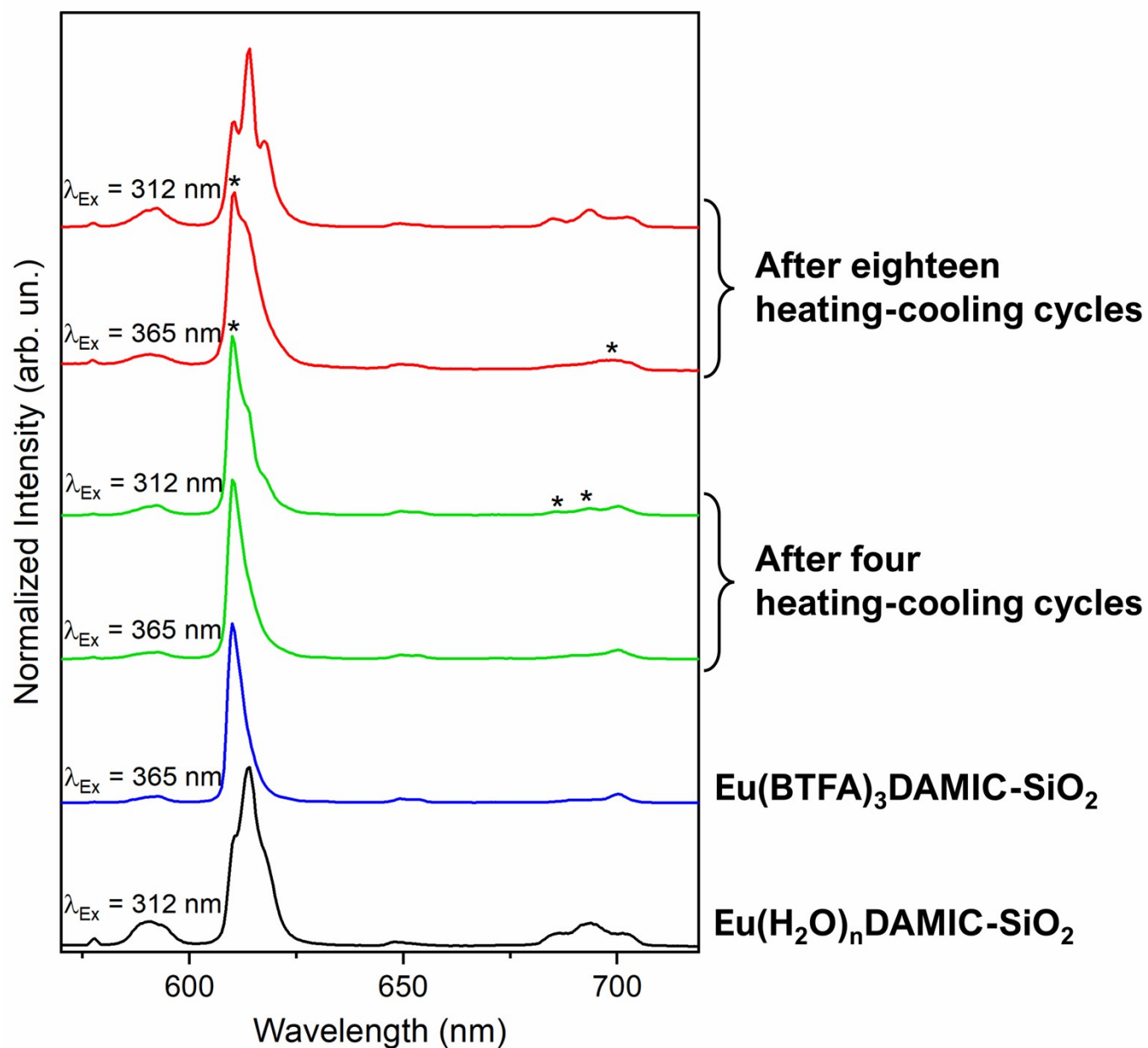


Figure S18. Emission spectra of the UFPE label before, after soak with BTFA and after heating cycles.

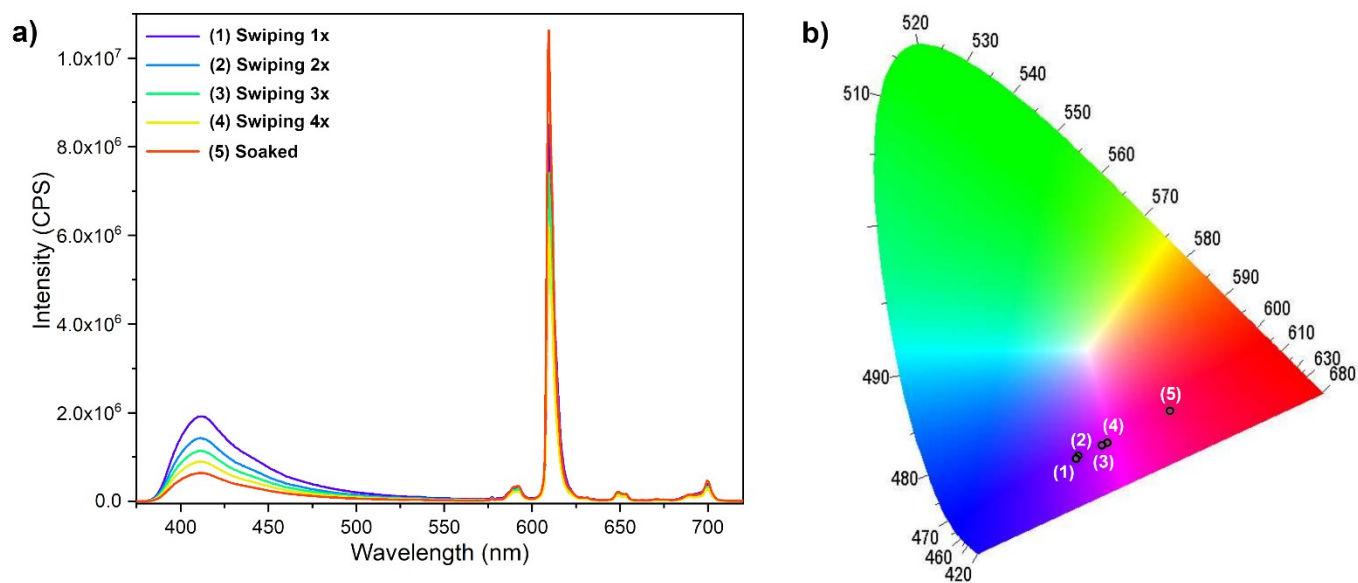


Figure S19. Emission spectra of the UFPE label before and after successive addition of the BTFA solution with the marker pen.

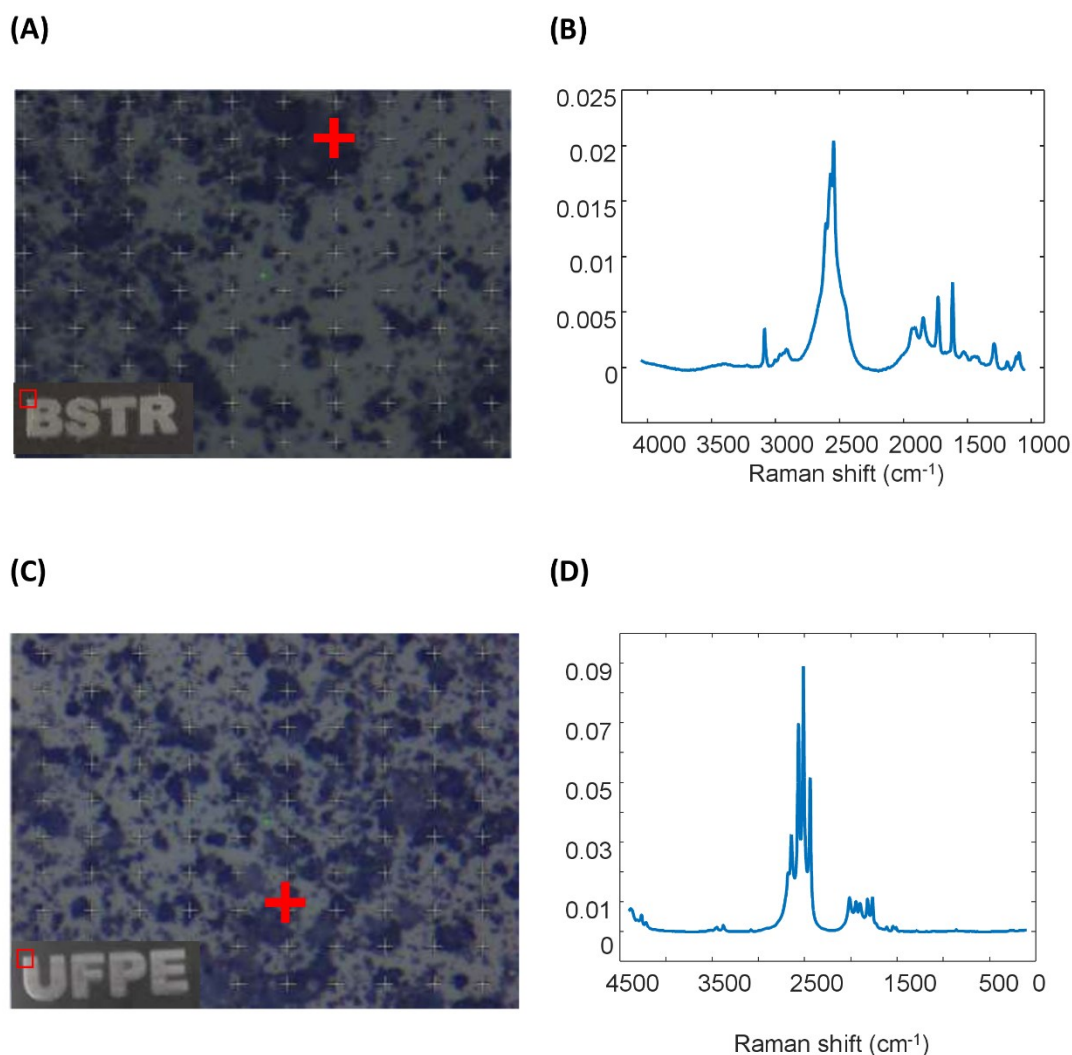


Figure S20. Images of (a) EuDAMIC-MCM48 and (c) EuBTC-MCM48 using magnification of 50x and the respective Raman spectra acquired (b) and (d) using the 532 nm laser.

REFERENCES

- 1 Q. Li, Z. Wang, D.-M. Fang, H. Qu, Y. Zhu, H. Zou, Y. Chen, Y.-P. Du and H. Hu, *New J. Chem.*, 2014, **38**, 248–254.
- 2 M. et al Fujiwara, *acsnano*, 2008, **2**, 1671–1681.
- 3 T.-W. Kim, P.-W. Chung and V. S.-Y. Lin, *Chem. Mater.*, 2010, **22**, 5093–5104.
- 4 A. N. Carneiro Neto, E. E. S. Teotonio, G. F. de Sá, H. F. Brito, J. Legendziewicz, L. D. Carlos, M. C. F. C. Felinto, P. Gawryszewska, R. T. Moura, R. L. Longo, W. M. Faustino and O. L. Malta, 2019, pp. 55–162.
- 5 K. Liu, H. You, Y. Zheng, G. Jia, L. Zhang, Y. Huang, M. Yang, Y. Song and H. Zhang, *CrystEngComm*, 2009, **11**, 2622.

- 6 K. Song, H. Yu, J. Zhang, Y. Bai, Y. Guan, J. Yu and L. Guo, *Crystals*, 2020, **10**, 185.
- 7 D. Y. Medina-Velazquez, B. Y. Alejandro-Zuniga, S. Loera-Serna, E. M. Ortiz, A. de J. Morales-Ramirez, E. Garfias-Garcia, A. Garcia-Murillo and C. Falcony, *J. Nanoparticle Res.*, 2016, **18**, 352.
- 8 Q.-F. Li, D. Yue, W. Lu, X. Zhang, C. Li and Z. Wang, *Sci. Rep.*, 2015, **5**, 8385.
- 9 I.Y. Li and B. Yan, *J. Mater. Chem.*, 2011, **21**, 8129